Available online at www.sciencedirect.com
ScienceDirect
Trans. Nonferrous Met. Soc. China 30(2020) 472−483
Transactions of Nonferrous Metals Society of China
www.tnmsc.cn

Mechanical properties and friction−wear characteristics of VN/Ag multilayer coatings with heterogeneous and transition interfaces

Yong-qiang ZHAO[1], Yong-tao MU[1,2], Ming LIU[1]

1. School of Mechatronics Engineering, Harbin Institute of Technology, Harbin 150001, China;
2. Vehicle Engineering Center, Geely Automobile Research Institute,
Zhejiang Geely Holding Group Co. Ltd., Ningbo 315336, China

Received 28 May 2019; accepted 4 December 2019

Abstract: The heterogeneous multilayer interface of VN/Ag coatings and transition multilayer interface of VN/Ag coatings were prepared on Inconel 781 and Si(100), and the microstructures, mechanical and tribological properties were investigated from 25 to 700 °C. The results showed that the surface roughness and average grain size of VN/Ag coatings with transition multilayer interface are obviously larger than those of VN/Ag coatings with heterogeneous multilayer interface. The coatings with transition multilayer interface have higher adhesion force and hardness than the coatings with heterogeneous multilayer interface, and both coatings can effectively restrict the initiation and propagation of microcracks. Both coatings have excellent self-adaptive lubricating properties with a decrease of friction coefficient as the temperature increases, but their wear rates reveal a drastic increase. The phase composition of the worn area of both coatings was investigated, which indicates that a smooth Ag, Magnéli phase (V_2O_5) and bimetallic oxides (Ag_3VO_4 and $AgVO_3$) can be responsible to the excellent lubricity of both coatings. To sum up, the coatings with transition multilayer interface have excellent adaptive lubricating properties and can properly control the diffusion rate and release rate of the lubricating phase, indicating that they have great potential in solving the problem of friction and wear of mechanical parts.

Key words: VN/Ag multilayer coatings; heterogeneous multilayer interface; transition multilayer interface; tribological properties; friction temperature; oxides

1 Introduction

V-series oxides have a slippery shear surface and show excellent solid lubrication effect under friction [1]. The multilayer or multiphase structures formed by the combination of the VN phase with other grains or amorphous phases generally have excellent tribological properties and cutting performance. In addition, the composite materials formed by the combination of VN lattice and other lubrication phases have continuous self-lubricating properties in a wide temperature range, so VN-based composite coatings have become one of the frontier topics in the field of tribology [2].

VN coating is a widely-studied self-lubricating material for cutting tool, and its friction and wear characteristics in a wide temperature range have an important influence on the cutting performance and service life of the cutting tool [3−5].

Under the complicated working conditions of temperature change and oxidation of the cutting tool, the VN coatings do not have self-lubricating properties in the low-temperature range (below 200 °C), and the friction and wear characteristics under medium and high-temperature conditions (around 400 °C and above) are not ideal. By doping elements in the VN lattice, the hardness and wear

Foundation item: Project (51505100) supported by the National Natural Science Foundation of China
Corresponding author: Yong-qiang ZHAO; Tel: +86-451-86402462; E-mail: zhyq_hit@126.com
DOI: 10.1016/S1003-6326(20)65227-X

resistance of the structure can be improved [6−15]. In addition, the multilayer structure design of VN coatings can effectively control the release rate of the lubricating phase, improving the load-carrying capacity and service life of the coating [16−22]. However, the existing work mainly focuses on the doping of Al and Si elements in VN coatings, and cutting experiments of doping V elements [7,8,23]. The optimization of cutting performance and friction and wear characteristics of coatings is mainly realized by the comparison method, which is insufficient for the structural design and process selection of coatings.

VN/Ag multilayer coatings have excellent self-lubrication properties in a wide temperature range [24−28]. But, the research is not systematic and in-depth, and the mechanical and friction and wear characteristics of VN/Ag multilayer coatings with different interface characteristics have not been comparatively investigated.

In this work, the multilayer coatings of VN/Ag with heterogeneous and transition interfaces were prepared, and the element contents of the heterogeneous and transition interfaces of VN/Ag multilayer coatings were measured by energy dispersive spectrometer. Moreover, the influence mechanism of the two interface structures on the mechanical and tribological properties of the coatings was investigated and analyzed comprehensively over a wide temperature range.

2 Experimental

2.1 Coating deposition

The VN/Ag composite coatings with two interface characteristics were prepared on Inconel 718 and Si (100) substrates by multi-arc ion plating technique to sputter three V targets (99.99 wt.% in purity) and three Ag targets (99.99 wt.% in purity). The coatings were prepared in a pure nitrogen (99.99% in purity) atmosphere with a discharge of 350 mL/min, a substrate bias voltage of −100 V, a deposition temperature of 400 °C, and a working pressure of 5 Pa.

The VN/Ag composite coatings with heterogeneous and transition interfaces are denoted as VN/Ag coating 1 and VN/Ag coating 2, respectively. For VN/Ag coatings 1, the Ag target was first shut off, and the V target was turned on and held for 7 min at 60 A to form a VN layer. Then, the V target was shut off, and the Ag target was turned on and held for 3 min at 50 A to form an Ag layer. The VN layer and the Ag layer were set up as one block. The deposition was repeated 11 times to form the heterogeneous interface multilayer structure. For VN/Ag coating 2, the Ag target was also first shut off during deposition, and the V target was evaporated for 7 min at 60 A to form a VN layer, and then the state of the V target was kept unchanged and the VN/Ag layer was formed after co-deposition for 3 min, in which the Ag target current was firstly increased in the order of 30, 40 and 50 A, and then decreased by 40 and 30 A. The Ag target current was kept at 50 A for 1 min, while the other current gradients were kept for 30 s, so the Ag content of the VN/Ag layer was gradually decreased from symmetric cross-section to interface. The gradient VN/Ag layer and the VN layer were set up as one block. The deposition was repeated 11 times to form the transition interface multilayer structure. The design structures of the two coatings are shown in Fig. 1.

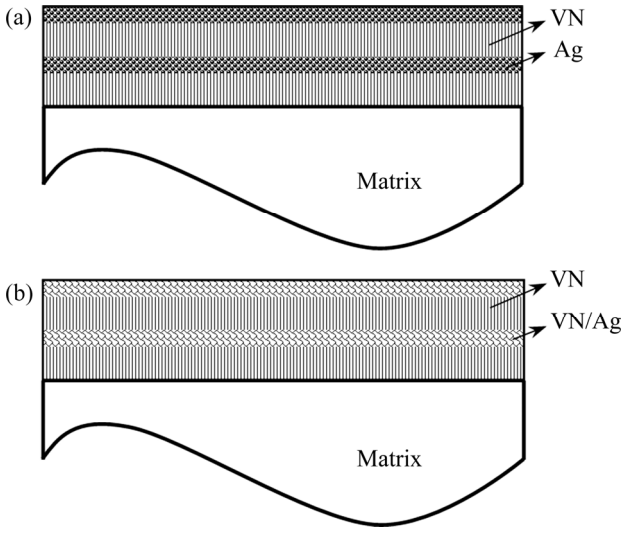

Fig. 1 Structural schematics for VN/Ag coating 1 (a) and VN/Ag coating 2 (b)

2.2 Characterization

The surface morphologies of the two composite coatings were characterized by a field emission scanning electron microscope (SEM), which was equipped with an energy dispersive spectroscopy system (EDS) for elemental analysis. The surface roughness of the coating was measured using an atomic force microscope (AFM) and the microstructure was identified by an X-ray diffractometer (XRD). The adhesion force (LC) was

detected using a scratch tester (CSM Instruments Revetest, Switzerland). The hardness of the coating was tested by a Vickers microhardness tester (MVS−1000D1) equipped with an indenter using a quadrangular pyramid diamond with an edge angle of 136°. The load applied to the sample by the indenter was 3 N, and the Vickers hardness value was calculated as follows:

$$H=0.1891F/d^2 \quad (1)$$

where H is Vickers hardness (MPa), F is the test force (N), and d is the arithmetic mean value of two diagonal lines of indentation (mm).

The indentation area of the Vickers hardness test was cut longitudinally using a focused ion beam cutting equipment (FIB, Carl Zeiss, Auriga). The surface morphology and cutting section morphology of the indentation area were observed using the dual-beam (ion beam and electron beam) scanning electron microscope attached to the FIB system. The tribological properties of two VN/Ag multilayer coatings were tested by a ball-on-disk tribometer (CETR UMT−3, USA), the relative humidity was (58±5)% and the room temperature was about (25±2) °C. The test parameters were as follows: normal load 10 N, test time 30 min, sliding speed 100 r/min, diameter of sliding track 6 mm, at room temperature, 300, 500 and 700 °C with a 10 mm Al_2O_3 ball as the counterpart.

3 Results and discussion

3.1 Morphology of VN/Ag 1 and VN/Ag 2 coatings

The surface morphologies and EDS results of VN/Ag 1 and VN/Ag 2 coatings are shown in Fig. 2. It can be seen from Fig. 2(a) that the surface of the VN/Ag coating 1 is laterally flattened by a plurality of columnar micro-nano particles, while the surface of the VN/Ag coating 2 is relatively compact and smooth (Fig. 2(b)). In addition, many tapered particles are scattered on the surfaces of the two coatings. As shown in Fig. 2(c), the EDS test results of the VN/Ag coating 1 show that the columnar and tapered particles on the surface contain abundant Ag elements. That is, the Ag content is 46 wt.%, and the contents of the V and N elements are 21 wt.% and 29 wt.%, respectively. For VN/Ag coating 2 (Fig. 2(d)), the EDS analysis shows that the Ag content on the surface and in particles of the

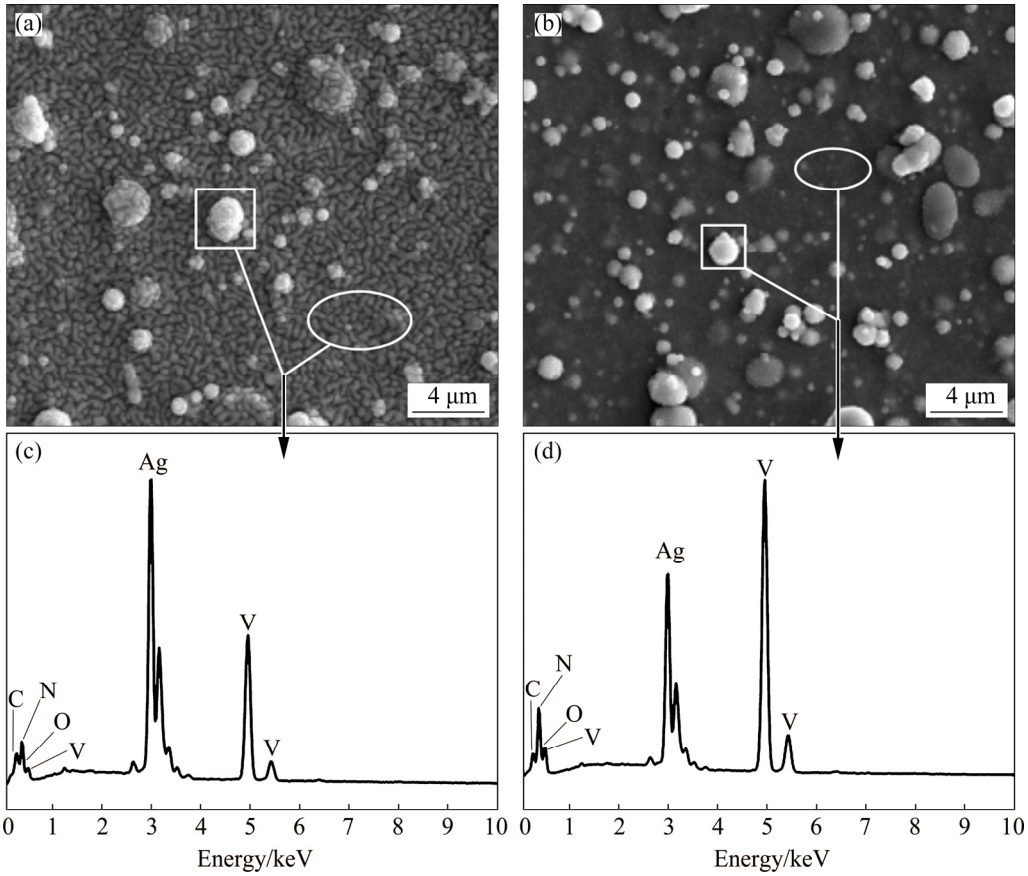

Fig. 2 SEM images (a, b) and EDS results (c, d) of VN/Ag coating 1 (a, c) and VN/Ag coating 2 (b, d)

sample decreases significantly, while the relative content of the V element increases significantly. The specific contents of Ag, V, and N are 24, 36 and 31 wt.%, respectively. It can be observed that the content of Ag element decreases with respect to the Ag layer of the VN/Ag coating layer 1, the content of the V element increases, and the content of the N element basically remains unchanged.

Figure 3 shows the surface morphologies of VN/Ag coating 1 and VN/Ag coating 2 measured by atomic force microscopy. According to the test results, the surface roughness of VN/Ag coating 1 is 214 nm, while that of VN/Ag coating 2 is 263 nm, which is 23% higher than that of the former.

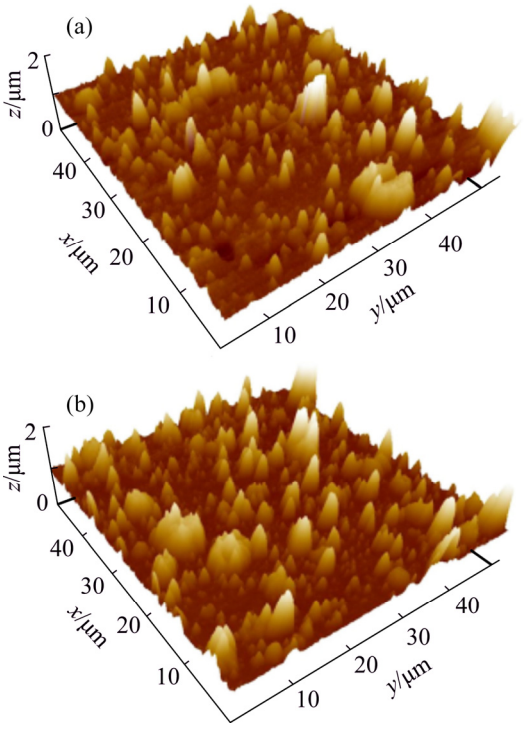

Fig. 3 Surface roughness of VN/Ag coating 1 (a) and VN/Ag coating 2 (b)

The X-ray diffraction patterns of VN/Ag coating 1 and VN/Ag coating 2 are shown in Fig. 4. Obviously, the two coatings have obvious diffraction peaks at about 2θ=33.8°,38.2°, 44.3°, 64.4°, 77.4°, and 81.7°. Compared with the XRD standard spectrum, these diffraction peaks correspond to crystal planes of Ag_2O (111) and VN/Ag phases (111), (200), (220), (311) and (222). As shown in Fig. 4, the diffraction peak intensity of the Ag_2O (111) increases significantly in the VN/Ag coating 2 compared with the VN/Ag coating layer 1, while the diffraction peak intensity of VN/Ag

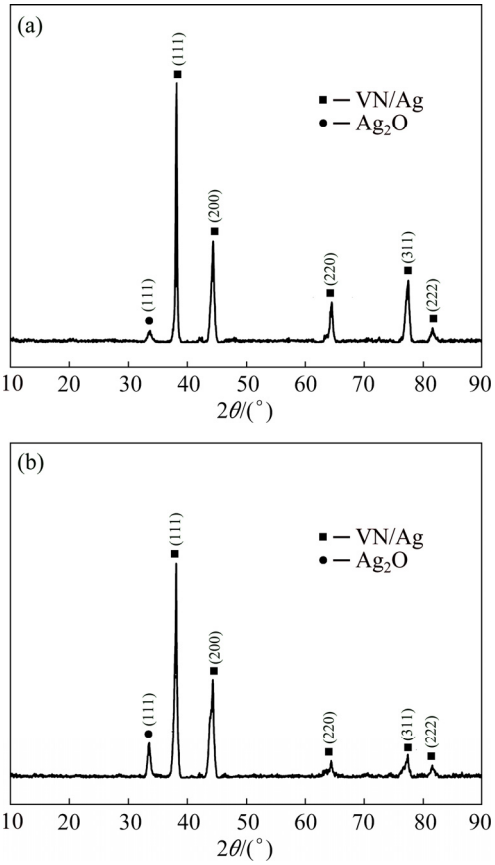

Fig. 4 XRD patterns of VN/Ag coating 1 (a) and VN/Ag coating 2 (b)

phases decreases, especially, that of the VN/Ag (111) close-packed surface. The increase of the diffraction peak intensity of the Ag_2O (111) crystal plane indicates that the VN/Ag coating 2 has relatively low oxidation resistance, while the decrease of the diffraction peak intensity of the VN/Ag phases is mainly attributed to the grain coarsening of the VN/Ag coating 2. The grain size of VN/Ag coating 1 and VN/Ag coating 2 is calculated by

$$D=K\lambda/(\beta\cos\theta) \quad (2)$$

where D is the average grain size (nm), K is the Scherrer constant (K=0.89), λ is the X-ray wavelength, β is the diffraction peak half-width and θ is the Bragg angle (°). The average grain size of VN/Ag coating 1 is 9.8 nm, while that of VN/Ag coating 2 is 11.9 nm. Obviously, the average grain size of VN/Ag coating 2 is 21% larger than that of VN/Ag coating 1.

3.2 Mechanical properties of VN/Ag 1 and VN/Ag 2 coatings

Figure 5 shows the results of the adhesion

force of VN/Ag coating 1 and VN/Ag coating 2. For the VN/Ag coating 1, as shown in Fig. 5(a), when the scratch length is 0.4 mm and the scratch depth is 5 μm, the acoustic emission signal of the sample first appears as a sharp peak, while the corresponding contact load is 15 N. This characteristic indicates that the VN/Ag coating 1 has a large degree of exfoliation or cracking. During the subsequent loading process, the acoustic signal is relatively stable under other loads except for a small fluctuation near 30 and 86 N, which indicates that the subsequent loading does not cause a large degree of damage to the coating. Therefore, the adhesion force of VN/Ag coating 1 is 15 N. For the VN/Ag coating 2, as shown in Fig. 5(b), when the scratch length is 0.3 mm and the scratch depth is 7 μm, the acoustic signal of the sample fluctuates for the first time, and the contact load at this time is 21 N. When the scratch length of the sample is larger than 1.1 mm and the scratch depth is larger than 22 μm, the amplitude of acoustic signal fluctuation increases obviously. When the scratch length is 2.8 mm and the scratch depth is 39 μm, the amplitude of acoustic emission signal fluctuation reaches the maximum, and the contact load is 168 N. It can be observed that the sample has an initial crack at a load of 21 N, and the critical load is 21 N. When the contact load is 71 N, the surface of the sample is exfoliated obviously, and when the load increases to 168 N, the crack further expands, which leads to a large area exfoliation of the coating, so the critical load of the VN/Ag coating 2 is 71 N. From scratch test results, it can be seen that the co-deposition of V and Ag targets at different currents can effectively inhibit the initiation and propagation of cracks in the coating and improve the bonding strength between the coating and the substrate when preparing gradient layer of VN/Ag coating 2.

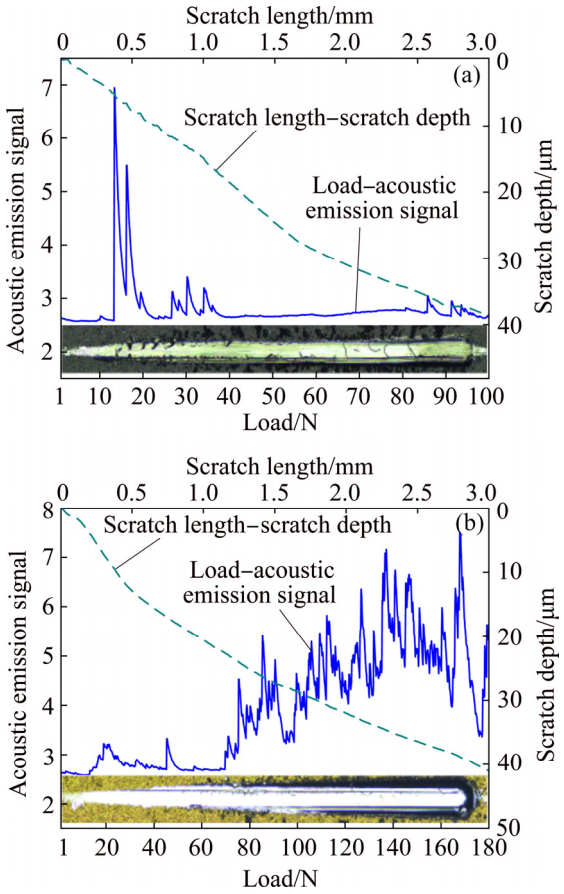

Fig. 5 Scratch test results of VN/Ag coating 1 (a) and VN/Ag coating 2 (b)

The indentation surface and FIB cutting section morphology of VN/Ag coating 1 and VN/Ag coating 2 are shown in Fig. 6. As shown in Figs. 6(a, b), the geometric dimensions of the indentation of the VN/Ag coating 1 are significantly larger than the corresponding value of the VN/Ag coating 2 under loading conditions of 3 N. By calculation, the Vickers microhardness values of the two coatings are $HV_{0.3}$180 and $HV_{0.3}$208, respectively. Obviously, the Vickers hardness of VN/Ag coating 2 is higher than that of VN/Ag coating 1. Furthermore, the cross-sectional morphologies of Figs. 6(c, d) show that both coatings have an obvious multilayer structure. However, the interdigitated layers of VN/Ag coating 1 result in the discontinuity of the interface between VN and Ag layers. In addition, the longitudinal cracks generated under indentation load obviously distribute in multiple modulation periods of the coating, wherein the largest-size crack is located at the boundary of the indentation zone, which is mainly caused by the stress concentration subjected to the bending load, while the other cracks are mainly attributed to the failure of the coating caused by the uneven deposition or uneven loading. For the VN/Ag coating 2, the indentation section shows that the intermittently deposited Ag particles distribute uniformly along the tangential direction of the surface in the VN crystal, and the vertical growth thickness of each gradient VN/Ag layer is consistent. However, under normal loading conditions, obvious longitudinal cracks also appear in the coating around the deposition defects.

3.3 Tribological properties of VN/Ag 1 and VN/Ag 2 coatings

The friction coefficients of VN/Ag coating 1 and VN/Ag coating 2 sliding against Al_2O_3 ball in ambient air at room temperature (RT) and high temperature are presented in Fig. 7. At room temperature, the stable friction coefficient of VN/Ag coating 1 (Fig. 7(a)) is 0.56, while that of VN/Ag coating 2 (Fig. 7(b)) is 0.50. The friction coefficient of the gradient transition interface multilayer structure is lower than that of alternating heterogeneous interface multilayer structure, which is mainly attributed to the plastic deformation of the Ag layer on the surface of VN/Ag coating 1. The surface layer of VN/Ag coating 2 has a solid solution structure formed by VN lattice and Ag particles, which has a high yield strength during the rubbing process so that the friction interface can be kept relatively flat and smooth. The friction coefficients of the two coatings change obviously at 300 °C, and the friction coefficient of VN/Ag coating 1 decreases to 0.44, while the measured value of VN/Ag coating 2 increases significantly to 0.57. The decrease of the friction coefficient of VN/Ag coating 1 is mainly attributed to the enhanced lubrication of the Ag layer under high-temperature conditions, and the increase in the measured value of VN/Ag coating 2 can be attributed to the higher roughness of the coating surface caused by hard VN phase. At 500 °C, the

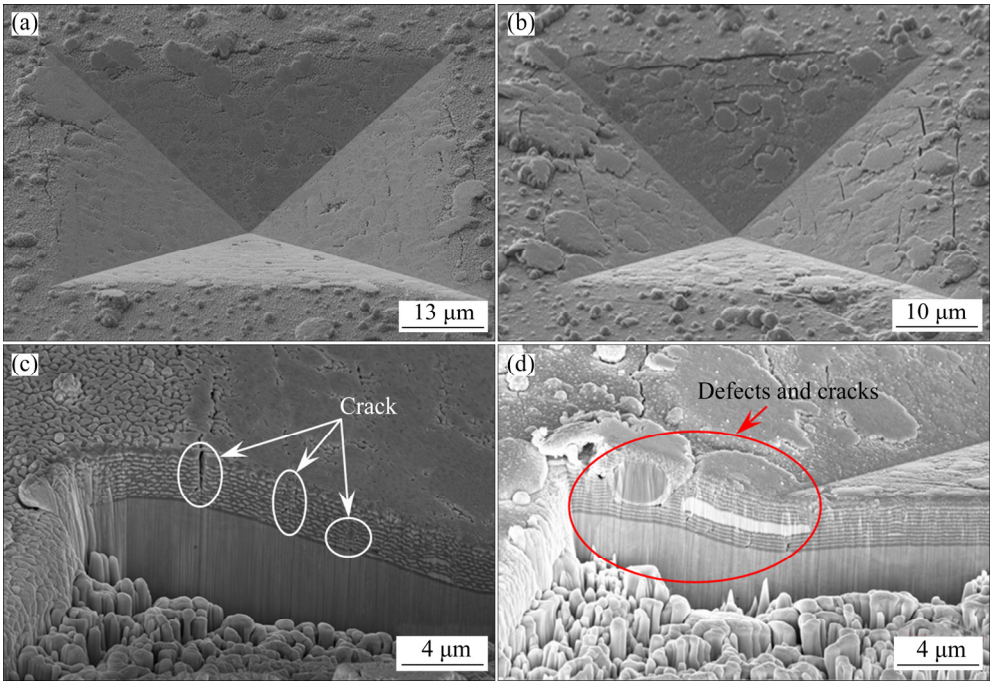

Fig. 6 Indentation (a, b) and its section using FIB incision (c, d) of VN/Ag coating 1 (a, c) and VN/Ag coating 2 (b, d)

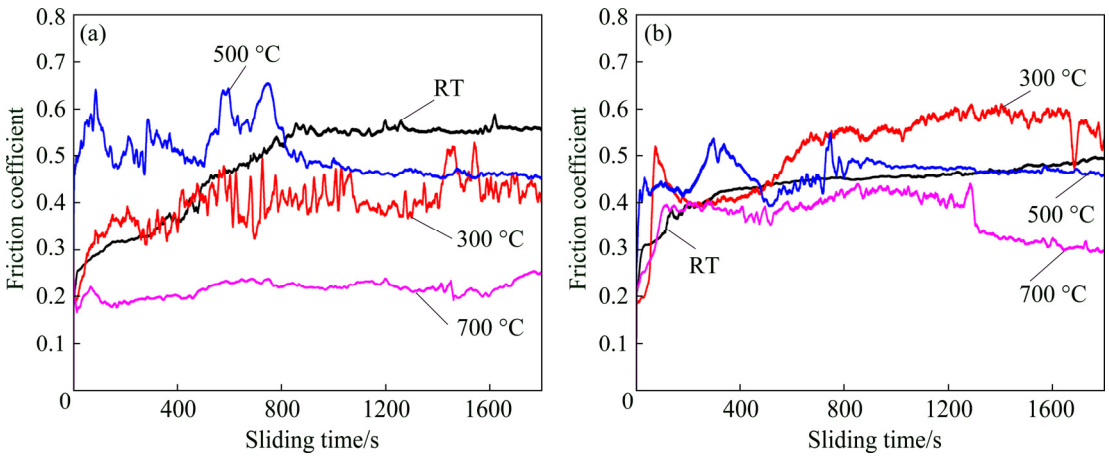

Fig. 7 Friction coefficients of VN/Ag coating 1 (a) and VN/Ag coating 2 (b) at different temperatures

stable friction coefficients of the two coatings tend to be close, namely 0.45 and 0.46, respectively. At this temperature, oxidation of the sample has an important effect on the lubrication of the friction interface. The V element is easily oxidized to V_2O_5 of the Magnéli phase at a high temperature of 500 °C. In addition, the oxide of the V element reacts with the metal Ag to form vanadate and metavanadate of Ag element, which can effectively lubricate the friction interface of coating and Al_2O_3 ball.

The friction coefficients of the two coatings reach the minimum value at 700 °C, i.e., for VN/Ag coating 1, the minimum value is 0.22, and for VN/Ag coating 2, the minimum value is 0.30. Obviously, the friction coefficient of the alternating heterogeneous interface multilayer coating is lower than that of the gradient transition interface multilayer coating, which is contrary to the measured results at room temperature. The main reason is that the friction interface has a completely different lubrication mechanism at two test temperatures. At room temperature, the two coatings are mainly lubricated by the Ag phase, while at 700 °C, the oxidation of Ag_3VO_4, $AgVO_3$, and V_2O_5 produced by oxidation reaction and tribochemical reaction plays an active role in reducing the friction coefficient of the samples. In addition, $AgVO_3$ and V_2O_5 have a lower melting point, and they can change the lubrication state of friction interface from solid lubrication to liquid lubrication at 700 °C. However, due to the controlling effect of the VN phase on the diffusion and release of Ag particles, the bimetallic oxides produced by VN/Ag coating 2 are relatively few, so the friction coefficient of VN/Ag coating 2 is slightly higher at 700 °C.

The wear morphologies of the two VN/Ag composite coatings sliding against Al_2O_3 balls at different temperatures are shown in Fig. 8. At room temperature, the friction surface of VN/Ag coating 1 (Fig. 8(a)) is comparatively smooth and flat, but there is much transfer wear debris piling up on both sides of the wear track. The wear mechanism is mainly attributed to the low bonding strength of the metal Ag layer and ceramic VN layer at the heterogeneous interface, resulting in delamination and spalling under the action of the tangential force. In addition, the surface Ag layer has lower hardness and yield strength, so the coating has lower wear resistance under shearing force. For VN/Ag composite coating 2, as shown in Fig. 8(b), the wear debris on the wear surface and both sides of the wear track is relatively small, and the radial width of the wear track is significantly reduced. These characteristics indicate that the wear resistance of VN/Ag coating 2 is higher at room temperature. The main reason is that the solid solution formed by the metal Ag phase and the ceramic VN phase improves the adhesion force and shear resistance of the coating. The radial wear width of VN/Ag coating 1 (Fig. 8(c)) increases significantly when the temperature rises to 300 °C, while the wear debris on the wear surface and both sides of the wear track decreases significantly. For VN/Ag coating 2 (Fig. 8(d)), the radial width of wear track increases greatly, and the wear debris on both sides of the wear track increases significantly. In addition, the wear debris forms a friction layer during the relative sliding process, and the circumferential stripes distributed on the friction layer show that the sample and the grinding ball are subjected to abrasive wear during relative movement. Under the friction condition of 500 °C, the wear morphology of VN/Ag coating 1 (Fig. 8(e)) shows a large change, the wear width is further increased, the abrasive debris accumulating on both sides of the wear track greatly increases, and the particle size is obviously increased. In addition, the frictional surface is characterized by the sweep of melting substances, which is mainly attributed to the formation of $AgVO_3$ inorganic salts by VN/Ag coating 1 at high temperatures. For VN/Ag coating 2 (Fig. 8(f)), the wear track morphology, radial wear width, geometry and dimension of wear debris are similar to those of VN/Ag coating 1, which indicates that the two coatings have the same friction and wear mechanism at 500 °C. The friction surfaces of both coatings show rough morphologies at 700 °C (Figs. 8(g, h)), which are mainly attributed to the formation, melting and solidification of oxidation products such as $AgVO_3$ and V_2O_5 on the surface of the samples.

In order to further analyze the friction and wear mechanism of two VN/Ag composite coatings sliding against Al_2O_3 ball in ambient air, the wear morphologies of Al_2O_3 balls matching VN/Ag coatings at different friction temperatures are shown in Fig. 9. As shown in Figs. 9(a, b), at room temperature, there is a small amount of transfer

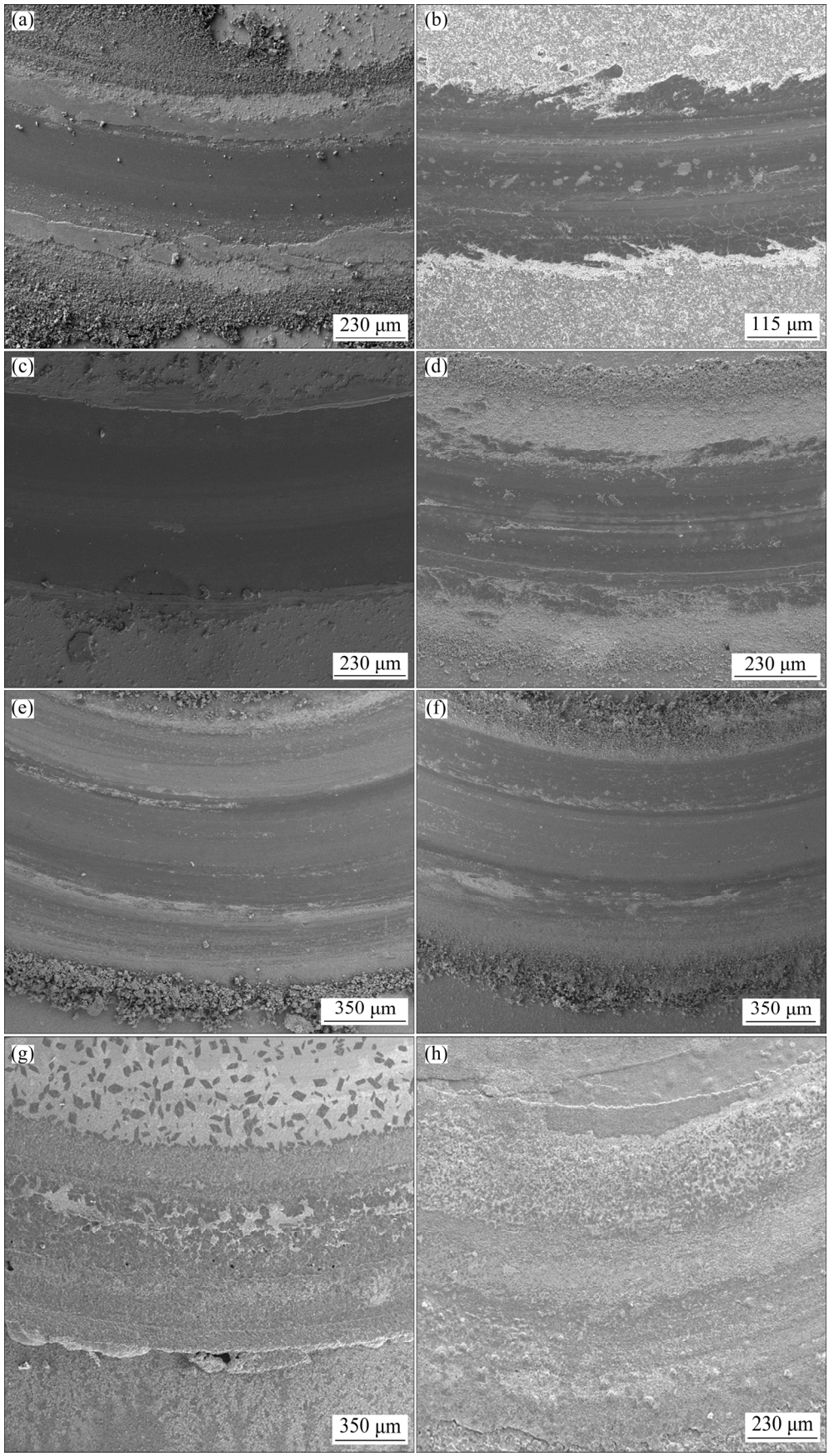

Fig. 8 Wear morphologies of VN/Ag coating 1(a, c, e, g) and VN/Ag coating 2(b, d, f, h) at different temperatures: (a, b) Room temperature; (c, d) 300 °C; (e, f) 500 °C; (g, h) 700 °C

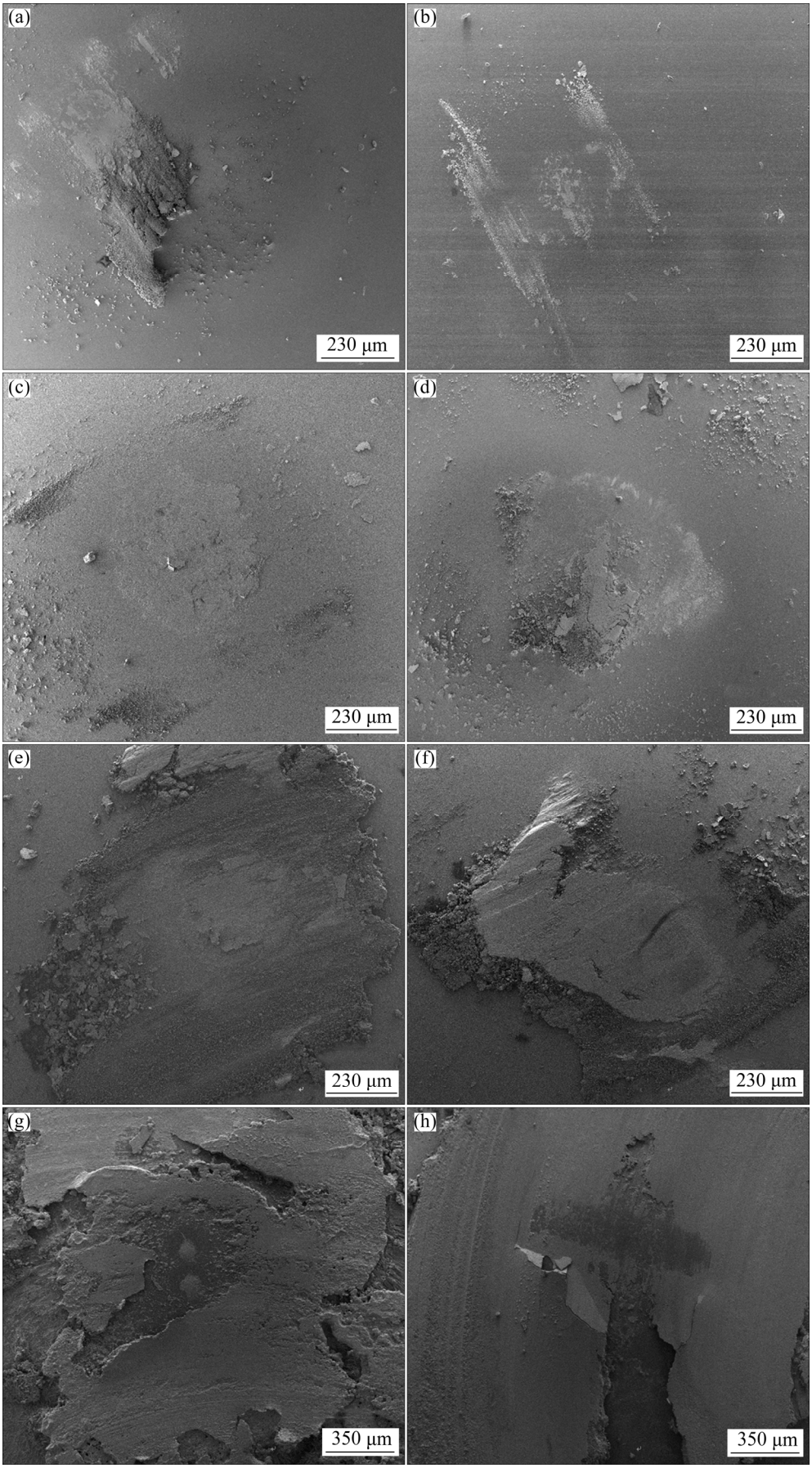

Fig. 9 Wear morphologies of Al_2O_3 balls matched with VN/Ag coating 1(a, c, e, g) and VN/Ag coating 2(b, d, f, h) at different temperatures: (a, b) Room temperature; (c, d) 300 °C; (e, f) 500 °C; (g, h) 700 °C

debris on the surface of Al_2O_3 grinding balls matched with both coatings, but there are no obvious wear characteristics on the surface of Al_2O_3 grinding balls.

At 300 °C, the wear morphologies of grinding balls matching VN/Ag coating 1 show a distinct circle (Fig. 9(c)), which is mainly the friction layer formed by the wear debris during the relative sliding process. For the grinding balls of VN/Ag coating 2 (Fig. 9(d)), the wear products of the friction surfaces show loose characteristics, and the dispersed debris usually acts as hard abrasive grains during the friction process, which results in serious particle wear. When the friction temperature rises to 500 °C, the number of transfer particles adhered to Al_2O_3 balls increases significantly. For VN/Ag coating 1 (Fig. 9(e)), transfer debris is laid on the friction surface of the counterpart ball, while for VN/Ag coating 2 (Fig. 9(f)), the thickness of transfer layer is obviously uneven, wherein the front ball surface of the contact area along the circumferential sliding direction accumulates more wear debris and the rear ball surface accumulates less wear debris. At 700 °C, as shown in Figs. 9(g, h), the wear products of the two pairs of grinding balls surface are condensed into a massive morphology, and the area and thickness of the transfer layer are significantly increased. These characteristics are consistent with corresponding coating morphologies, that is, they are mainly attributed to the formation and melting of the oxidation products at high temperatures, as well as the cooling and solidification of melted products at low temperatures.

3.4 Worn surface phase composition of VN/Ag 1 and VN/Ag 2 coatings

The micro-Raman spectra of the coatings with heterogeneous and transition interfaces sliding against Al_2O_3 balls at 500 and 700 °C are shown in Fig. 10. For VN/Ag coating 1, as shown in Fig. 10(a), the Raman spectra have obvious characteristic peaks at 397, 717, 837 and 921 cm^{-1} when the friction temperature is 500 °C, while when the friction temperature rises to 700 °C, the position of characteristic peaks changes to 357, 763, 836 and 894 cm^{-1}. For VN/Ag coating 2, as shown in Fig. 10(b), the characteristic peaks of Raman spectra at 500 °C are located at 483, 735, 821 and 933 cm^{-1}, while at 700 °C, the Raman peaks shift to 372, 763, 850, 924 and 989 cm^{-1}. From the Raman scattering characteristics of the two coatings, it can be observed that the oxidation reaction and tribochemical reaction of the friction interface between the sample and the Al_2O_3 ball generate oxides of V element and bimetallic oxides of Ag_3VO_4 and $AgVO_3$ during the relative sliding process. The characteristic peaks of Raman spectra of both coatings are detected at 717 and 821 cm^{-1} at 500 °C, which correspond to Ag_3VO_4 vanadate of Ag.

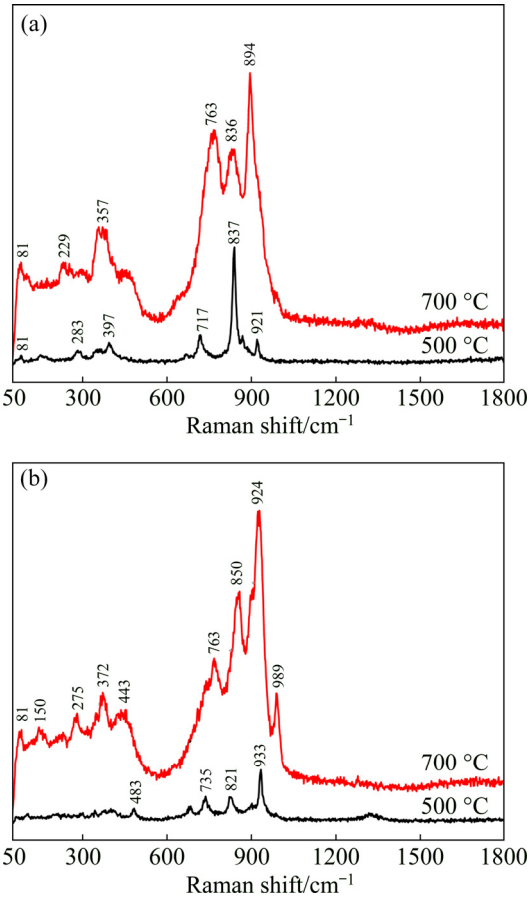

Fig. 10 Raman spectra of VN/Ag coating 1 (a) and VN/Ag coating 2 (b) at high temperatures

In the crystal structure of the Ag_3VO_4 phase, the weak Ag—O and Ag—Ag bonds have lower shear resistance, so the Ag_3VO_4 phase can provide good lubrication under high-temperature test under the friction load. In addition, the V_2O_5 oxide has a Magnéli phase structure, and its slip surface with low shear strength also has an effective anti-friction effect at 500 °C. However, Ag_3VO_4 vanadate has lower thermochemical stability, and as the temperature increases, it decomposes into the meta-vanadate of Ag, namely $AgVO_3$ and elemental

Ag. Therefore, at 700 °C, the wear surface of the two coatings has a Raman peak of $AgVO_3$ metavanadate, and corresponding peaks are located at 357, 763, 894 and 924 cm^{-1}. Both $AgVO_3$ and V_2O_5 have a lower melting point. Therefore, at a friction temperature of 700 °C, the friction interface between the coating and the Al_2O_3 ball changes from solid lubrication to liquid lubrication.

4 Conclusions

(1) The intermittence gradient Ag-doped structure of the VN phase has larger surface roughness, average grain size and lower oxidation resistance compared with the heterogeneous interface multilayer structure of the Ag and VN phase.

(2) The multilayer structure formed by the VN phase and VN/Ag solid solution has higher adhesion force and hardness than that of the VN−Ag multilayer structure.

(3) The friction coefficient of the transition interface multilayer coatings is relatively low at room temperature, but relatively high at 300 and 700 °C. In addition, the measured values of the two coatings are similar at 500 °C.

(4) The oxides of V_2O_5, Ag_3VO_4 and $AgVO_3$ formed through the tribochemical reactions play a critical role in the improving lubrication properties of both coatings. The transition multilayer interface of VN/Ag coatings exhibits improved adaptive lubricating properties as compared to the heterogeneous interface VN/Ag coatings by properly controlling the diffusion rate and release rate of the lubricating phase.

References

[1] SU Q, LIU X Q, MA H L, GUO Y P, WANG Y Y. Raman spectroscopic characterization of the microstructure of V_2O_5 films [J]. J Solid State Electr, 2008, 12: 919−923.

[2] GE Fang-fang, ZHU Ping, MENG Fan-ping, XUE Qun-ji, HUANG Feng. Achieving very low wear rates in binary transition-metal nitrides: The case of magnetron sputtered dense and highly oriented VN coatings [J]. Surface and Coatings Technology, 2014, 248: 81−90.

[3] GASSNER G, MAYRHOFER P H, KUTSCHEJ K, MITTERER C, KATHREIN M. A new low friction concept for high temperatures: Lubricious oxide formation on sputtered VN coatings [J]. Tribology Letters, 2004, 17: 751−756.

[4] FALLQVIST M, OLSSON M. The influence of surface defects on the mechanical and tribological properties of VN-based arc-evaporated coatings [J]. Wear, 2013, 297: 1111−1119.

[5] FATEH N, FONTALVO G A, GASSNER G, MITTERER C. Influence of high-temperature oxide formation on the tribological behaviour of TiN and VN coatings [J]. Wear, 2007, 262: 1152−1158.

[6] POLÁKOVÁ H, MUSIL J, VLČEK J, ALLAART J, MITTERER C. Structure-hardness relations in sputtered Ti−Al−V−N films [J]. Thin Solid Films, 2003, 444: 189−198.

[7] KATHREIN M, MICHOTTE C, PENOY M, POLCIK P, MITTERER C. Multifunctional multi-component PVD coatings for cutting tools [J]. Surface and Coatings Technology, 2005, 200: 1867−1871.

[8] PFEILER M, KUTSCHEJ K, PENOY M, MICHOTTE C, MITTERER C, KATHREIN M. The influence of bias voltage on structure and mechanical/tribological properties of arc evaporated Ti−Al−V−N coatings [J]. Surface and Coatings Technology, 2007, 202: 1050−1054.

[9] KUTSCHEJ K, MAYRHOFER P H, KATHREIN M, POLCIK P, MITTERER C. Influence of oxide phase formation on the tribological behaviour of Ti−Al−V−N Coatings [J]. Surface and Coatings Technology, 2005, 200: 1731−1737.

[10] SCHNÖLLER J, FRANZ R, MITTERER C, HUTTER H. TOF-SIMS depth profiling and element mapping on oxidized AlCrVN hard coatings [J]. Analytical and Bioanalytical Chemistry, 2009, 393: 1857−1861.

[11] FRANZ R, SCHNÖLLER J, HUTTER H, MITTERER C. Oxidation and diffusion study on AlCrVN hard coatings using oxygen isotopes ^{16}O and ^{18}O [J]. Thin Solid Films, 2011, 519: 3974−3981.

[12] BOBZIN K, BAGCIVAN N, EWERING M, BRUGNARA R H, THEIß S. DC-MSIP/HPPMS (Cr,Al,V)N and (Cr,Al,W)N thin films for high-temperature friction reduction [J]. Surface and Coatings Technology, 2011, 205: 2887−2892.

[13] FRANZ R, NEIDHARDT J, KAINDL R, SARTORY B, TESSADRI R, LECHTHALER M, POLCIK P, MITTERER C. Influence of phase transition on the tribological performance of arc-evaporated AlCrVN hard coatings [J]. Surface and Coatings Technology, 2009, 203: 1101−1105.

[14] MU Yong-tao, LIU Ming, ZHAO Yong-qiang. Carbon doping to improve the high temperature tribological properties of VN coating [J]. Tribology International, 2016, 97: 327−336.

[15] KUANG Hai, TAN Dun-qiang, HE Wen, YI Zhi-qiang, YUAN Fan, XU Yu-kun. Oxidation behavior of the TiAlN hard coating in the process of recycling coated hardmetal scrap [J]. RSC Advances, 2019, 9: 14503−14510.

[16] ZHOU Z, RAINFORTH W M, RODENBURG C, HYATT N C, LEWIS D B, HOVSEPIAN P E. Oxidation behavior and mechanisms of TiAlN/VN coatings [J]. Metallurgical and Materials Transactions A, 2007, 38: 2464−2478.

[17] MAYRHOFER P H, HOVSEPIAN P E, MITTERER C, MÜNZ W D. Calorimetric evidence for frictional self-adaptation of TiAlN/VN superlattice coatings [J]. Surface and Coatings Technology, 2004, 177−178: 341−347.

[18] LUO Q. Origin of friction in running-in sliding wear of

nitride coatings [J]. Tribology Letters, 2010, 37: 529−539.
[19] ZHOU Z, RAINFORTH W M, LUO Q, HOVSEPIAN P E, OJEDA J J, ROMERO-GONZALEZ M E. Wear and friction of TiAlN/VN coatings against Al_2O_3 in air at room and elevated temperatures [J]. Acta Materialia, 2010, 58: 2912−2925.
[20] KAMATH G, EHIASARIAN A P, PURANDARE Y, HOVSEPIAN P E. Tribological and oxidation behaviour of TiAlCN/VCN nanoscale multilayer coating deposited by the combined HIPIMS/(HIPIMS-UBM) technique [J]. Surface and Coatings Technology, 2011, 205: 2823−2829.
[21] HOVSEPIAN P E, EHIASARIAN A P, PETROV I. TiAlCN/VCN nanolayer coatings suitable for machining of Al and Ti alloys deposited by combined high power impulse magnetron sputtering/unbalanced magnetron sputtering [J]. Surface Engineering, 2010, 26: 610−614.
[22] HOVSEPIAN P E, KAMATH G, EHIASARIAN A P, HAASCH R, PETROV I. Microstructure, oxidation and tribological properties of TiAlCN/VCN coatings deposited by reactive HIPIMS [C]//IOP Conference Series: Materials Science and Engineering. Bristol, England: IOP Publishing Ltd, 2012, 39: 012011.
[23] KUTSCHEJ K, MAYRHOFER P H, KATHREIN M, POLCIK P, MITTERER C. Influence of oxide phase formation on the tribological behaviour of Ti−Al−V−N coatings [J]. Surface and Coatings Technology, 2005, 200: 1731−1737.
[24] AOUADI S M, SINGH D P, STONE D S, POLYCHRONOPOULOU K, NAHIF F, REBHOLZ C, MURATORE C, VOEVODIN A A. Adaptive VN/Ag nanocomposite coatings with lubricious behavior from 25 to 1000 °C [J]. Acta Materialia, 2010, 58: 5326−5331.
[25] MU Yong-tao, LIU Ming, WANG Yong-xin, LIU Er-yong. PVD multilayer VN-VN/Ag composite coating with adaptive lubricious behavior from 25 to 700 °C [J]. RSC Advances, 2016, 6: 53043−53053.
[26] GUO Hong-jian, HAN Min-min, CHEN Wen-yuan, LU Cheng, LI Bo, WANG Wen-zhen, JIA Jun-hong. Microstructure and properties of VN/Ag composite films with various silver content [J]. Vacuum, 2017, 137: 97−103.
[27] GUO Hong-jian, LU Cheng, ZHANG Zhen-yu, LIANG Bu-nv, JIA Jun-hong. Comparison of microstructures and properties of VN and VN/Ag nanocomposite films fabricated by pulsed laser deposition [J]. Applied Physics A, 2018, 124: 694.
[28] FU Tao, ZHANG Zi-jian, PENG Xiang-he, WENG Sha-yuan, MIAO Yu-han, ZHAO Yin-bo, FU Shao-yun, HU Ning. Effects of modulation periods on mechanical properties of V/VN nanomultilayers [J]. Ceramics International, 2019, 45: 10295−10303.

异质及过渡界面 VN/Ag 多层涂层的力学性能及摩擦磨损特性

赵永强[1]，慕永涛[1,2]，刘 明[1]

1. 哈尔滨工业大学 机电工程学院，哈尔滨 150001；
2. 浙江吉利控股集团有限公司 吉利汽车研究院 车辆研究中心，宁波 315336

摘 要：利用多弧离子镀技术在 Inconel 718 和 Si(100)基体上沉积异质及过渡界面 VN/Ag 多层涂层，对其在 25~700 °C 的显微组织、力学性能和摩擦学性能进行研究。结果表明：过渡 VN/Ag 多层涂层的表面粗糙度及平均晶粒尺寸比异质界面 VN/Ag 多层涂层的明显增大。过渡 VN/Ag 多层涂层比异质界面 VN/Ag 多层涂层具有更高的结合力及硬度，两种涂层均可以有效抑制微裂纹的萌生及扩展。两种涂层均具有优异的协同润滑效应，随着温度的升高，摩擦因数降低，但磨损率却急剧增加。两种涂层摩擦表面的物相研究表明：Ag、V_2O_5、Ag_3VO_4 和 $AgVO_3$ 对涂层良好的润滑性能起到至关重要的作用。综上所述，VN/Ag 涂层的过渡层界面具有良好的自适应润滑性能，能够适当控制润滑相的扩散速率和释放速率，因此，在解决机械零件的摩擦磨损问题上具有很大的潜力。

关键词：VN/Ag 复合涂层；异质多层界面；过渡多层界面；摩擦学性能；摩擦温度；氧化物

(Edited by Bing YANG)